SPE 89393

X-Ray Computed Microtomography Studies of Disproportionate Permeability Reduction

R. S. Seright, SPE, New Mexico Petroleum Recovery Research Center, **Masa Prodanovic**, and W**. Brent Lindquist**, SPE, State University of New York at Stony Brook

Abstract

X-ray computed microtomography (XMT) was used to understand why a Cr(III)-acetate-HPAM gel reduced permeability to water 80-90 times more than that to oil in strongly water-wet Berea sandstone and in strongly oil-wet porous polyethylene. During oil flow after gel placement in Berea, a 55% (average) reduction in gel volume occurred in pores of all detected size ranges, thus leading to a relatively high permeability to oil. In porous polyethylene, reduction in gel volume occurred mainly in small pores. Because the first oil injection after gel placement did not reduce gel volume to a greater extent in large pores than in small pores, the reduction in gel volume was probably caused by gel dehydration rather than by gel ripping or extrusion.

The overall S_{or} in Berea jumped from 18.4% before gel placement to 51% after. The greater level of trapped oil greatly restricted water flow. Before gel placement, most residual non-wetting blobs were isolated within individual pores. In Berea at S_{or} after gel placement, the largest residual oil blob was 122 times larger than the largest oil blob at S_{or} before gel placement. This high degree of connectivity for the oil phase explains the relatively high permeability to oil after gel placement. This large blob may exist because gel affinity for water limited the formation of water films that were needed to break the large oil blob into small blobs.

In porous polyethylene, the overall S_{or} was significantly lower after gel placement than before gel placement (0.3% versus 17.0%). Thus, oil trapping could not explain the large disproportionate permeability reduction (F_{rrw}/F_{rro}=89). Gel dehydration and rehydration provide a viable explanation. In particular, paths may open during oil injection by partial dehydration of the gel. During subsequent water injection, the paths could partially close when the gel rehydrates.

Introduction

In previous work,[1,2] X-ray computed microtomography (XMT) was used to understand why gels reduce permeability to water more than that to oil. That work revealed that "strong" Cr(III)-acetate-HPAM gels formed in virtually all aqueous pore spaces. For normal pressure gradients, water injected after gel placement was forced to flow through the gel itself, experiencing microdarcy permeabilities. In contrast, even for relatively low pressure gradients, oil injection destroyed gel or reduced the gel volume so as to enhance oil permeability (relative to water flow). During subsequent water flow (after oil flow and after gel placement), the gel trapped much higher levels of residual oil (relative to the S_{or} before gel placement)—thus, again providing a permeability to water that was much less than that to oil. Two major questions from the previous work were (1) how does oil injection destroy or reduce the volume of the gel and (2) how does the gel trap larger volumes of residual oil? This paper addresses these questions using a new analysis called "indicator kriging," which was superior to our former method to distinguish between phases in a given XMT image. The XMT method and subsequent analysis were used to follow fluid saturations in individual pores during various flooding stages in strongly water-wet Berea sandstone and strongly oil-wet porous polyethylene. The flooding stages included (1) oil and water injection cycles before gel placement, (2) gelant placement, and (3) oil and water injection cycles after gel placement.

We had several motivations to re-examine our previous XMT data. First, the earlier analysis found that the smallest detected pores in strongly water-wet Berea sandstone had lower average water saturations at S_{or} and S_{wr} then expected from conventional wisdom. Second, especially in Berea, a newly developed method was superior in distinguishing between oil, water, and rock on a microscopic level. Third, although our first analysis obtained saturations for individual pores throughout various flooding stages, it did not indicate how extensively oil or water were connected from pore to pore. In other words, it did not indicate the sizes of water and oil "blobs". In contrast, our new analysis was able to quantify phase connectivity.

Our ultimate goal in these studies is to identify ways to maximize disproportionate permeability reduction in a predictable and controllable manner.

Differences between the Old and New Analyses

Procedural Differences. In our first analysis,[1,2] assignment of the locations of rock, water, and oil voxels were made as follows. First, rock locations were identified from images of cores that were saturated only with the wetting phase. These rock locations were used in subsequent images to pin down the liquid-filled pore space. Second, fluid phase identification was made by subtracting an image having both fluid phases present (one phase of which was doped with a strong X-ray attenuating compound) from the corresponding image in which only the wetting phase was present in the pore space. A histogram of the subtracted X-ray attenuation coefficients showed a bimodal distribution—the peaks in the distribution corresponding to water- and oil-filled voxels. The subtracted image contained significantly greater overlap between the peaks than an unsubtracted image. There were several reasons for overlap between the peaks in the histogram:

1) The finite size of a voxel means that any X-ray attenuation coefficient measured is an average over the voxel volume.
2) Variations in X-ray counting statistics result in variations in attenuation coefficients.
3) Minor alignment errors occur, of ~1/2-1 voxel width.

While 1) and 2) affect peak overlap in non-subtracted images, in subtracted images their influence is exacerbated. Item 3) contributes for subtracted images, but not unsubtracted ones.

In the first analysis, simple thresholding was used to distinguish water-and oil-filled voxels.[1,2] The threshold was determined from the bimodal subtraction histogram, with the threshold value picked to lie in the "valley'" between the two peaks. Simple thresholding is well known to result in speculated images (i.e., apparent blobs of one phase trapped in the other). The extent of the speculation is proportional to the overlap between the two peaks in the difference histogram.

In the newer analysis, rock locations determined from single-phase flooded core images were still used in subsequent images of the two-phase flooded core to identify the liquid-filled space. However, the subtraction procedure was not used. Rather, a segmentation procedure based upon indicator kriging was used to segment the phases in the pore space only. This avoided any artificial spreading induced by a subtraction procedure. Additionally, the indicator kriging method does not rely on global thresholding, but performs local segmentation based upon maximum likelihood decisions. The result is a cleaner resolution of the fluid phases.

The basic idea of kriging is to estimate an unknown random variable (e.g., the "true" X-ray attenuation value of a voxel) by a linear combination of known random variables (i.e., measured attenuation values) plus a possible systematic shift. The data values, however, are not assumed to be independent (as in classical linear regression analysis) but are correlated spatially. The estimate is required to be unbiased, and the variance of the error in the estimate is required to be minimized. This leads to a constrained minimization problem, whose solution follows from a "constrained normal" system of linear equations known as the ordinary kriging system. While ordinary kriging estimates the value of the random variable at a point, indicator kriging gives the probability that the value at the point is greater than some threshold value. This probability then "indicates" the possible state (pore space or rock) at the point. Indicator kriging does so by capitalizing on the proportion of neighboring data valued above the same threshold, and accounts for the proximity of each datum to the unsampled location.

Differences in Results. A detailed comparison of the results from the old (first) and new (second) analyses can be found in Ref. 3. Here, we simply summarize the differences. First, the second analysis revealed larger pores in polyethylene (because a larger population was sampled—1,879 versus 308 pores). Second, the second analysis showed lower S_{wr} and S_{or} in Berea, which was more consistent with floods in larger cores. Third, the second analysis showed many more pores at high and low saturations in Berea than the first analysis. Fourth, in the transition from S_{wr} to S_{or}, many Berea pores gained oil in the first analysis but not in the second. Fifth, both analyses confirmed that S_{wr} averaged less than 60% in the smallest detected Berea pores and that a wide range of saturations could be found for any pore size. Finally, other trends were the same for both analyses. The remainder of this paper will focus on results obtained from the second analysis.

Experimental

A detailed description of the experimental studies was provided in Refs. 1 and 2. The aqueous Cr(III)-acetate-HPAM gel used in this work contained 0.5% Alcoflood 935 HPAM (~$5x10^6$ daltons, 5-10% degree of hydrolysis), 0.0417% Cr(III) acetate, 1% NaCl, and 0.1% $CaCl_2$. The brine contained 1% NaCl and 0.1% $CaCl_2$. The oil was hexadecane that was doped with either 10% iodohexadecane (used in Berea) or 15% bromohexadecane (used in polyethylene). All experiments were performed at room temperature except gelation, which occurred at ~60°C.

The Berea core (specifically, the "first Berea core" discussed in Ref. 1) had a permeability of 0.47 darcys and a porosity of 22%. The polyethylene core had a permeability of 8.8 darcys and a porosity of 40%. Fig. 1 compares the pore size distributions for Berea sandstone and porous polyethylene. The analyses examined 2,176 pores for the Berea sample and 1,879 pores for the polyethylene sample. The average pore size for polyethylene (0.00052 mm^3) was 44% greater than that for Berea (0.00035 mm^3). Interestingly, the median pore size was greater for Berea (0.00016 mm^3) than for polyethylene (0.00010 mm^3). The higher average for polyethylene occurred because it contained a larger fraction of pores with sizes greater than 0.002 mm^3 (compare the high end of the distributions in Fig. 1). Incidentally, if the pores were spherical (which they are not), the average pore radius would be 50 µm for polyethylene and 44 µm for Berea. XMT and scanning electron microscope images of the two samples can be found in Ref. 1.

Berea sandstone was first saturated with brine, while the porous polyethylene was first saturated with oil. Subsequently, cores were flooded with oil or water to establish residual water and oil saturations (S_{wr} and S_{or}, respectively). Next, gelant was injected and allowed to gel. After gel placement, cycles of oil and water were injected to establish S_{wr} and S_{or} conditions. XMT images were obtained after each flood. All floods and imaging were performed without removing the core from

ExxonMobil's X2B X-ray beamline at Brookhaven National Laboratory. Consequently, saturation changes can be followed for individual pores throughout the flooding sequences.
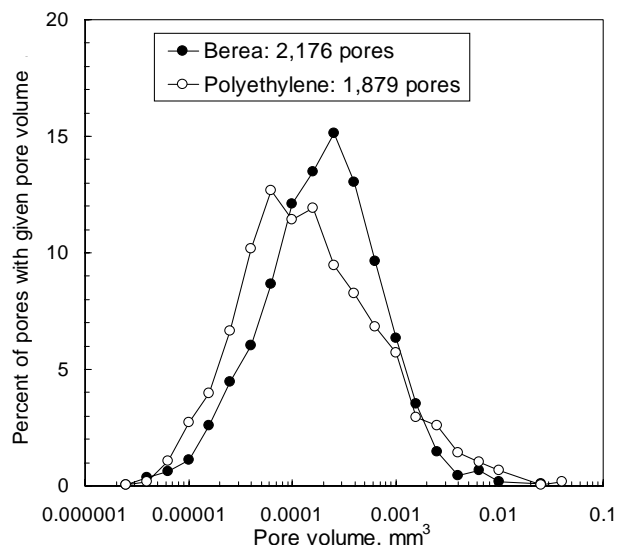

Fig. 1—Pore size distributions for Berea and polyethylene.

For each flooding stage, the water saturations versus pore size were compared. Table 1 summarizes the overall water saturations after each flooding step.

Table 1—Average water saturations after various floods.

	Berea	Polyethylene
@ S_{or1} before gel		86.0%
@ S_{wr} before gel	16.0%	16.5%
@ S_{or} or S_{or2}	81.6%	83.0%
@ Gel placement	63.7%	99.8%
@ S_{wr} after gel	28.7%	83.5%
@ S_{or} after gel	49.0%	99.7%

Saturations before Gel Placement

S_w Averaged <60% in the Smallest Detected Berea Pores. In Berea sandstone, the water saturation (S_w) averaged 16% at the connate water satuation (S_{wr}) before gel placement. The water saturations at S_{wr} are plotted in Fig. 2 for each of the 2,176 pores in Berea. The solid curve plots the average water saturation as a function of pore size. Note the large number of pores with very low (nearly zero) water saturation. At S_{wr}, 54.5% of the pores had $S_w < 5\%$. Water saturations near zero were common for pores in most size ranges. The solid curve suggests that the average water saturation in the smallest detected pores was less than 60%. However, few pores existed at the small end of the distribution, so an average value may not be particularly representative. Even so, it is clear that water saturations in the smallest pores were scattered over the entire range from 0 to 100%—just as in the other size ranges. On first consideration, this finding appears to contradict those who expect the water saturation to approach 100% in the smallest pores of a strongly water-wet porous medium. In reconciliation, pores may be present (especially in clays) that were smaller than we can detect with X-ray computed microtomography. (Our voxel size was 4.1 µm.) At any rate, the smallest detected pores ($\sim 5 \times 10^{-6}$ mm^3) in our analysis were confirmed to average less than 60% water saturation at S_{wr}.
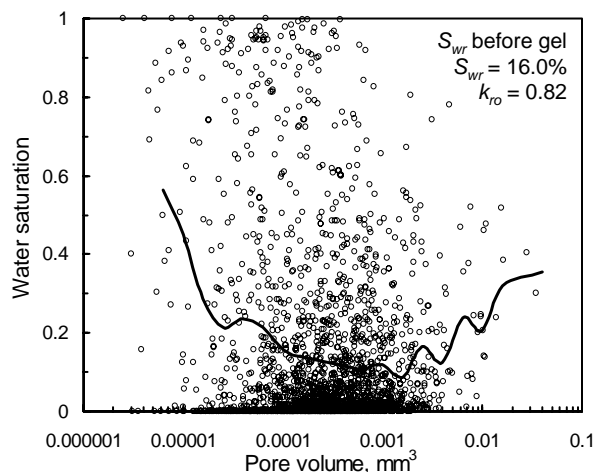

Fig. 2—Berea @ S_{wr} before gel.

Saturation Changes Were Insensitive to Berea Pore Size. Water saturations at the residual oil saturation (S_{or}) in Berea averaged 81.6% (Table 1), and the average was not sensitive to pore size (solid curve in Fig. 3). For all size ranges, note the large number of pores with high water saturations. At S_{or}, 39.4% of the pores had $S_w > 95\%$. During the transition from S_{wr} to S_{or} in Berea (Fig. 4 and compare Figs. 2 and 3), pores in all detected size ranges experienced significant gains in water saturation (averaging 65.6%). Pore size did not appear to significantly influence the extent of the transition. In a strongly water-wet porous medium, one might have expected smaller pores to experience smaller saturation changes.
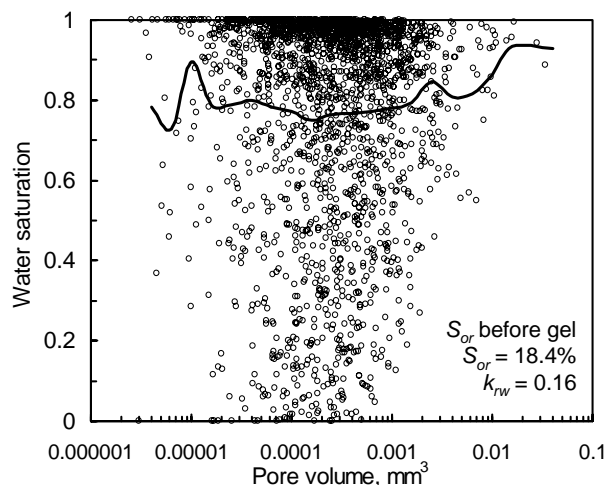

Fig. 3—Berea @ S_{or} before gel.

S_w Averaged <20% in the Smallest Polyethylene Pores. In porous polyethylene at the first residual oil saturation (S_{or1}), S_w averaged 86% (i.e., the oil saturation averaged 14%). The average water saturation in the smallest detected pores was less than 20% (Fig. 5). In other words, the wetting phase (oil) saturation averaged more than 80% in the smallest detected polyethylene pores. Recall that the wetting phase (water) saturation averaged less than 60% in the smallest detected Berea pores. For both porous media, the smallest detected pores were about the same size ($\sim 5 \times 10^{-6}$ mm^3). One might explain these observations by suggesting that the affinity of

polyethylene for oil was stronger than the affinity of sandstone for water. However, this suggestion is counter-intuitive since polar interactions between Berea minerals and water should be stronger than the non-polar interactions between polyethylene and hexadecane.
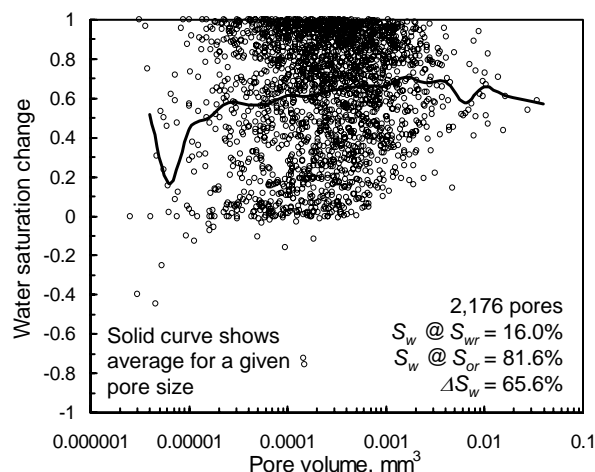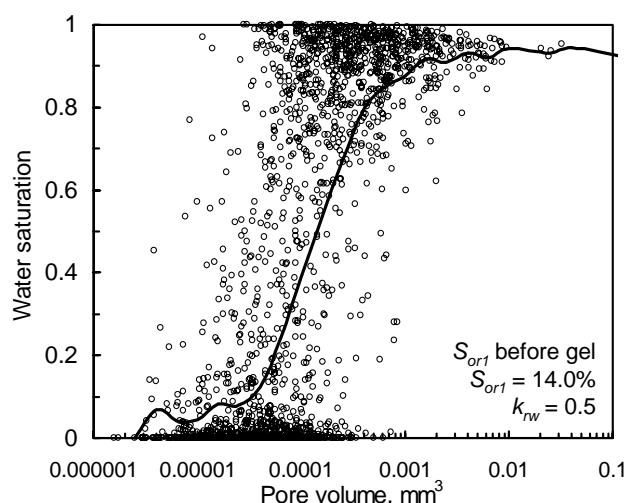

Fig. 4—Changes in Berea: S_{wr} to S_{or}.

Fig. 5—Polyethylene @ S_{or1} before gel.

Oil Was Largely Immobile in Small Polyethylene Pores. At S_{or} in polyethylene, most small pores had nearly 100% oil saturation, while most large pores had nearly 100% water saturation (Fig. 5). When oil was injected to drive the core to S_{wr} (Fig. 6), water was displaced from most medium to large pores so that most pores ended with nearly 100% oil saturation. When water was re-injected to drive the core to S_{or2}, most large pores again filled almost completely with water, while most small pores retained high oil saturations (Fig. 7). Interestingly, a complementary behavior was not seen in Berea. The pore and throat sizes in polyethylene were no smaller than those in Berea.[1,2]

Norman Morrow (University of Wyoming) offered a credible explanation why higher water satuations were not seen in the smallest detected Berea pores at S_{wr}. Berea pores were typically coated with kaolinite that significantly increased the surface roughness of the pore walls. In contrast, the pore walls in polyethylene were quite smooth (see Figs. 3

and 4 of Ref.1). At S_{or}, after oil drainage from the smooth polyethylene pore walls, an extremely thin (nanometer scale) oil film may have coated most pore walls (or possibly, no film may remain). At S_{wr} in strongly water-wet Berea, the rough clay coating made the effective thickness of the water film much greater than for any oil film in porous polyethylene. (We qualitatively noted this difference visually by close comparison of Figs. 10 and 11 of Ref. 1.) With a thicker effective wetting film, water drained fairly efficiently from the smallest detected Berea pores when oil was injected—thus allowing the smallest detected pores to reach water saturations comparable to those in larger pores (Fig. 2). In contrast, when water was injected into porous polyethylene, oil usually became hydraulically isolated in the smallest detected pores because any remaining wetting film was too thin to efficiently drain oil. Consequently, high oil saturations were usually seen in the smallest detected polyethylene pores (Figs. 5 and 7).
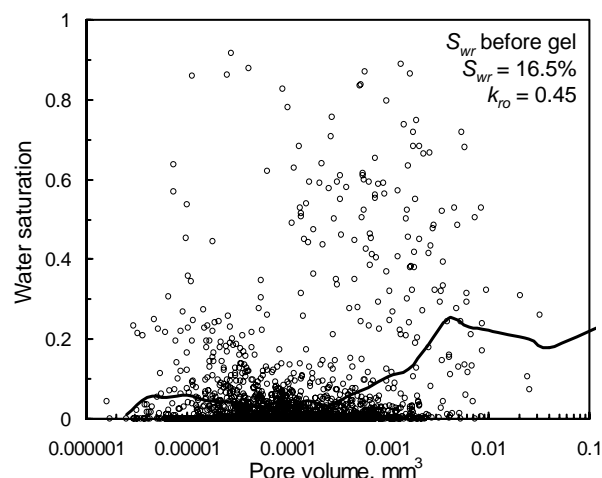

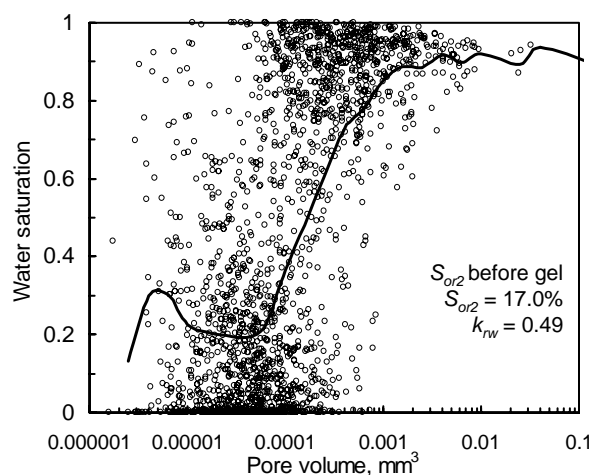**Fig. 6—Polyethylene @ S_{wr} before gel.**

Fig. 7—Polyethylene @ S_{or2} before gel.

20-cp Gelant Mobilized Oil in Both Porous Media
During gelant placement in Berea, the image volume surprisingly increased in oil saturation (from 18.4% to 36.3%). To rationalize this result, we note that the image volume was

located in the center of the core and was small compared to the total pore volume of the core. Oil from upstream of the image volume probably was mobilized by flow of the 20-cp gelant, and that oil coincidentally lodged in the image volume. The overall oil saturation in the core did not increase during gelant placement. Within the image volume, medium to large pores (10^{-4} to 10^{-2} mm^3) were most likely to gain in oil saturation (Fig. 8). Interestingly, the pressure gradient during gelant injection was always less than that during the previous brine or oil flows. This constraint was intentionally part of our experimental design to minimize oil mobilization. Since oil was mobilized, factors other than high pressure gradients were responsible for this mobilization.
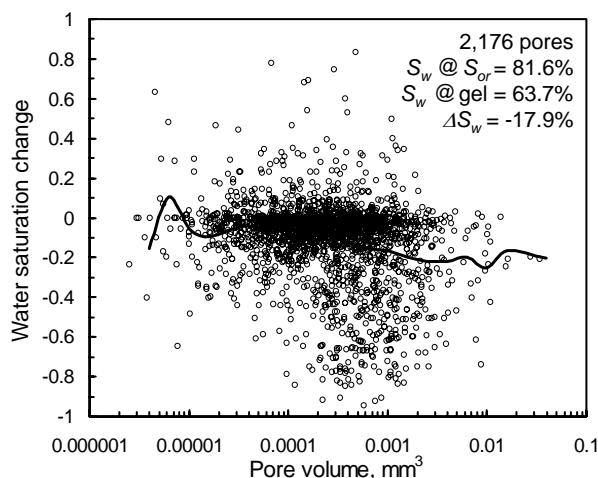

Fig. 8—Changes in Berea: S_{or} to gel placement.

During gelant placement in polyethylene, most oil that was trapped in small pores was displaced, so that most pores ended with high gelant saturations (compare Figs. 7 and 9). Only a few small pores retained large oil saturations (Fig. 9). The gelant or aqueous saturation increased from 83% to 99.8% during the process of gel placement (Table 1). As in Berea, the pressure gradient during gelant injection was always less than that during the previous brine or oil flows.
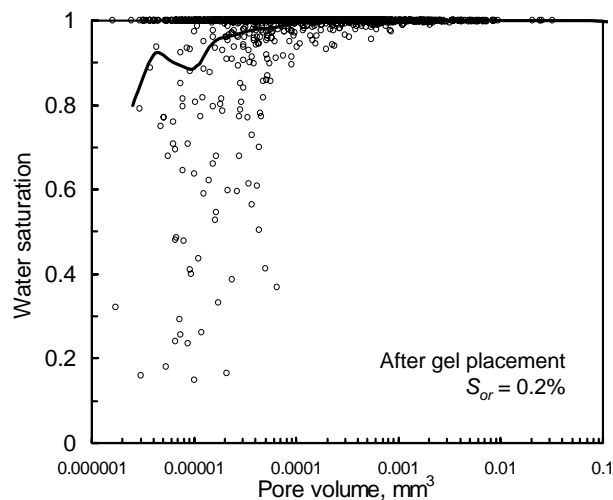

Fig. 9—Polyethylene after gel placement.

Why was oil mobilized from the small pores during gelant injection but not during the previous water injection—especially since the pressure gradient (35 psi/ft) during water injection was higher than during gelant injection? Could polymer or Cr(III) adsorption have altered the wettability (oil-wet to water-wet) of the polyethylene? This suggestion seems unlikely considering the hydrophobic nature of the surface and the hydrophilic nature of the polymer and crosslinker. Wang[4] suggested that viscoelastic forces associated with flow of polymer solutions may re-distribute forces on a microscopic scale so that oil may be mobilized. This explanation may also help explain oil mobilization during our Berea experiments. More work is needed to determine if this explanation is applicable for our polyethylene and Berea experiments.

Oil and Water Flooding after Gel Placement
Oil Injection Reduced Gel Volume in Berea. Perhaps the most important conclusion from our earlier work was that oil injection effectively reduced gel volume in many Berea pathways that were utilized by oil before gel placement.[1,2] This conclusion was confirmed by our new analysis. When gelant was placed, it effectively displaced all brine so that gel formed in all aqueous pore spaces. This observation was confirmed many times in previous work by noting that the Cr(III)-acetate-HPAM gel reduced Berea's permeability to water to levels associated with the permeability of the gel itself to water (i.e., water residual resistance factors of 10,000 or greater and final permeability in the microdarcy range).[5,6]

When oil was injected after gel formation, the oil saturation increased (by 35 saturation percentage points—see Table 1). Fig. 10 shows that most (95.2% of the total) pores gained oil (lost water) when oil was injected after gel placement. The effect of oil on the gel was not sensitive to pore size, since the average water saturation (solid curve in Fig. 10) decreased by about 35% regardless of pore size. Considering that the water saturation was 63.7% immediately before oil injection and 28.7% after oil injection, and assuming that gel occupied all of the aqueous pore space, the oil apparently destroyed (or reduced in volume) 55% of the gel. The pressure gradients during these experiments were limited so that they never exceeded those applied before the gel was placed. Therefore, it seems unlikely that the reduction in gel volume occurred because of exposure to excessive pressure gradients (i.e., extrusion of the gel from the core).

Fig. 11 provides additional insight into the process of reducing gel volume during oil injection. This plot shows the 300 pores (1/7 of total) that experienced the greatest increase in oil saturation during the process of oil injection after gel placement. Before gel placement, these pores were nearly full of oil at S_{wr} and were nearly full of water at S_{or}. Thus, oil and water both flowed freely into and filled these pores before gel placement. They were also easily accessible to oil after gel.

S_{wr} in Berea Was Higher after Gel Placement than before. Overall water saturation was higher at S_{wr} after gel placement (28.7%) than before gel placement (16.0%). (See Table 1 and Fig. 12.) From Fig. 12, 86.1% of the pores had higher S_{wr} values after gel placement than before gel. Presumably, gel accounted for this increase. (By itself, XMT cannot distinguish between water and gel.) In the previous section, we

estimated that oil injection reduced gel volume by 55%. Fig. 12 suggests that the remaining gel was widely distributed, although it was most likely to be found in medium to small pores. Fig. 12 also shows that few pores had lower S_{wr} values after gel placement than before gel.
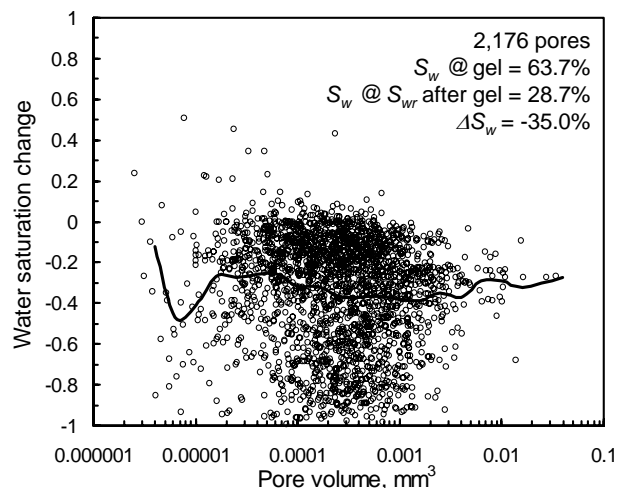
Evidentally, a significant degree of rearrangement occurred for water and oil saturations during this flood.

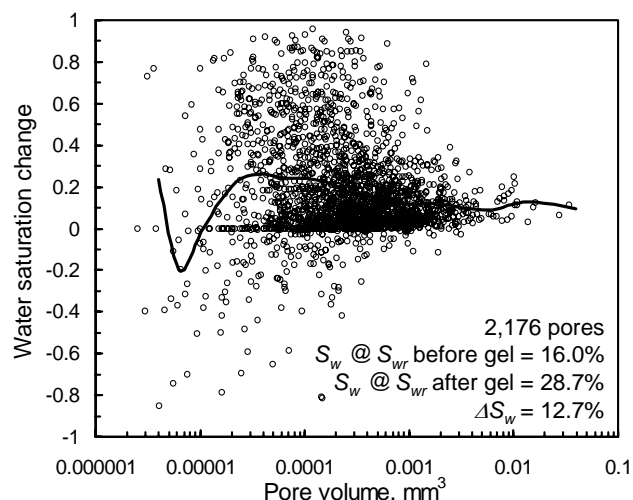**Fig. 10—Oil flooding to S_{wr} after gel placement in Berea.**

Fig. 12—Changes in Berea: S_{wr} before gel to S_{wr} after gel.

Fig. 11—Oil damaged gel most in pores that were easily filled by oil or water before gel.
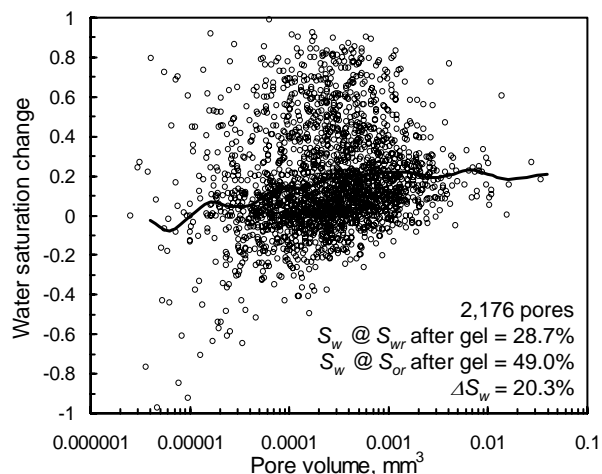
Fig. 13—Changes in Berea: S_{wr} after gel to S_{or} after gel.

On the other hand, many pores had nearly the same water saturation before and after gel placement (see the cluster of data points near zero change in water saturation in Fig. 12). In particular, 46% of the pores changed less than 10 saturation percentage points for the transition from S_{wr} before gel placement to S_{wr} after gel placement.

Oil Was Trapped in Berea during Subsequent Water Flow. During the transition from S_{wr} after gel placement to S_{or} after gel placement, the average increase in S_w was 20.3%. Fig. 13 reveals that a wide range of changes occurred for most pore sizes and the average saturation change was not particularly sensitive to pore size (although the average saturation changes were close to zero for the smaller pores). Interestingly, 22.6% of the pores gained oil even though water was injected.

During oil injection after gel placement, the oil residual resistance factor (F_{rro}, permeability reduction) was 15. During subsequent water injection, the water residual resistance factor (F_{rrw}) was 1,220. Thus, the gel reduced permeability to water 81 times more than to oil. As mentioned earlier, much of the gel was destroyed or reduced in volume during oil injection after gel placement. Why was the final permeability to water so much lower than that to oil? Previous analysis[1,2] indicated that the gel trapped significantly more residual oil. Our new analysis confirmed this conclusion, which indicated that S_{or} jumped from 18.4% before gel placement to 51% after gel placement (i.e., S_w decreased from 81.6% to 49%; see Table 1 and Fig. 14). With many pores permanently occupied by oil, water was forced to flow through narrow films and through the gel itself—explaining the large water residual resistance factor (i.e., 1,220). In contrast, oil pathways remained relatively free from constriction by the gel, so the oil residual resistance factor was much less (i.e., 15).
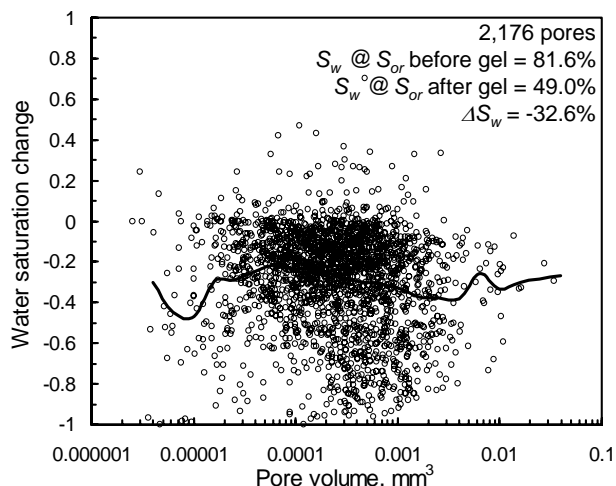
Fig. 14—Changes in Berea: S_{or} before gel to S_{or} after gel.

At S_{or} after gel placement, 93.3% of the pores had higher oil saturations than at S_{or} before gel placement. Fig. 14 reveals that a wide range of changes occurred for all pore sizes and that the average change was not sensitive to pore size.

In Polyethylene, Reduction of Gel Volume Occurred Mainly in Small Pores. As in Berea, gel appeared to form in all aqueous pore spaces of polyethylene (because permeability to water was in the µd range immediately after gel formation). When oil was injected after gel placement in polyethylene, the oil residual resistance factor was 24, and the overall S_{wr} value was 83.5% (Fig. 15). For comparison, the overall S_{wr} value was only 16.5% before gel placement (Fig. 6). Presumably, the difference (67 saturation percentage points) was due to gel that was not destroyed or dehydrated during oil injection. Put another way, oil injection reduced the gel volume by 16.3 saturation percentage points (99.8%-83.5%). This loss was substantially less than that seen in Berea (35 saturation percentage points from Table 1). If the losses could be attributed entirely to gel dehydration, the gel would have been concentrated by factors of 2.2 in Berea (i.e., 63.7/28.7) and only 1.2 in polyethylene (i.e., 99.8/83.5).
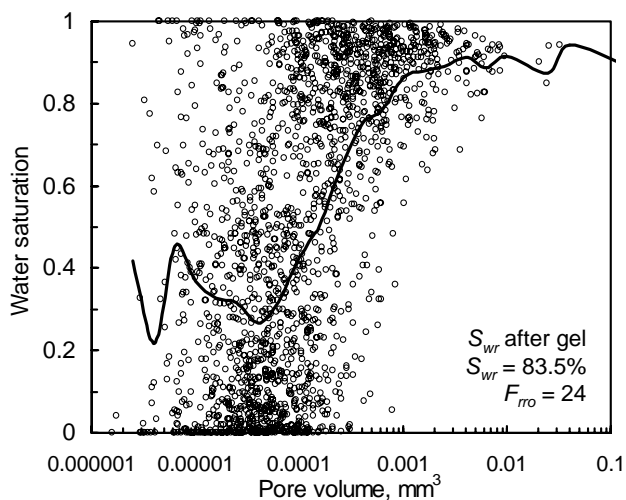

Fig. 15—Polyethylene @ S_{wr} after gel.

The oil saturation increased 63 saturation percentage points for pores that were smaller than 10^{-4} mm³ but only by 11 saturation percentage points for pores that were larger than 10^{-3} mm³ (see Fig. 16). Thus, compared to Berea, reduction of gel volume during oil injection into gel-filled porous polyethylene was more likely in small pores and less likely in large pores. As with our Berea experiments, the pressure gradients were not allowed to exceed 35 psi/ft during any stage of the polyethylene experiments. So again, it seems unlikely that reduction of gel volume occurred because of exposure to excessive pressure gradients. If high pressure gradients were responsible, gel damage should have been greater in larger pores than in smaller pores.

If the losses could be attributed entirely to gel dehydration, the gel would have been concentrated by factors of 2.8 in small polyethylene pores and 1.1 in large polyethylene pores.
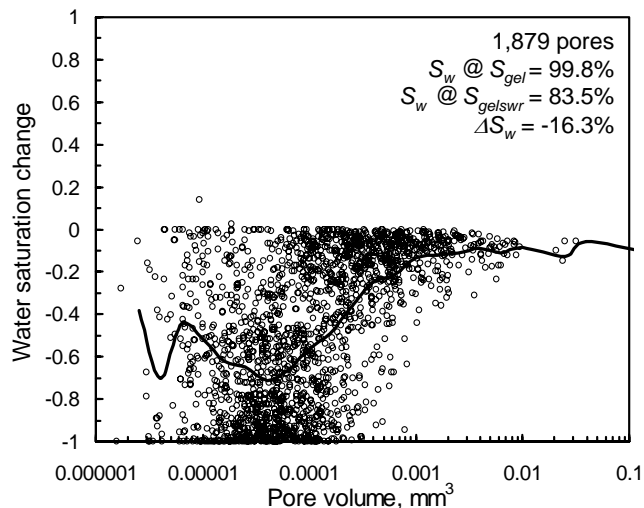

Fig. 16—Oil flooding to S_{wr} after gel placement in polyethylene.

In Polyethylene, S_{wr} after Gel Placement Looked Like S_{or} before Placement. A comparison of Figs. 5, 7, and 15 suggests that the saturation distributions at S_{wr} after gel placement in polyethylene were very similar to those at S_{or} before gel placement. Why should this similarity occur? Two factors contribute. First, as mentioned earlier, injected oil entered and destroyed (or reduced the volume of) gel preferentially in the small pores where residual oil was located before gel placement. Second, subsequently injected water displaced most oil from the smaller pores. (Since the larger pores were permanently filled with gel, no displacement apparently occurred in the larger pores.) It is interesting that water could displace oil from the small pores after gel placement but not before gel placement. As mentioned earlier, the pressure gradients for the post-gel floods were less than those for the pre-gel floods. Therefore, at present, we have no explanation for this behavior.

The oil residual resistance factor (F_{rro}) was 24. The mobile oil flow follows films and smallest pores. One might have expected much higher resistance to flow for low oil saturations and such narrow flow paths.

In Polyethylene, Additional Oil Was Not Trapped during Subsequent Water Injection. After the oil injection step associated with Fig. 16, water was injected to drive the core to S_{or}. The final saturations are plotted in Fig. 17. Notice the similarity between Figs. 9 and 17. In both cases, very little oil remained in the core (0.3% or less). The small oil saturation that was present generally existed in the smallest pores.
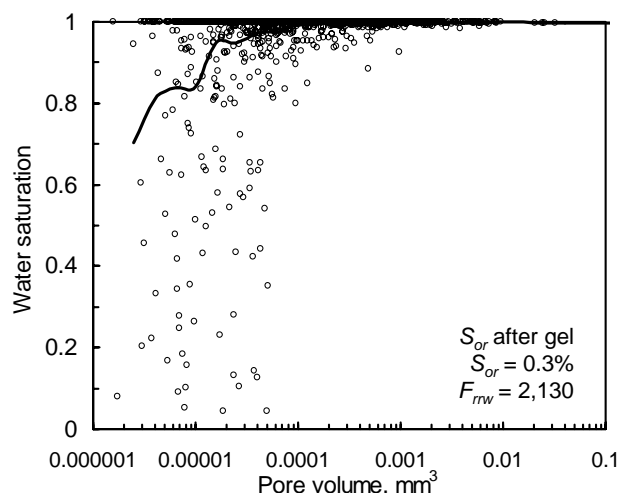

Fig. 17—Polyethylene @ S_{or} after gel.

The water residual resistance factor (F_{rrw}) was 2,130. Based on the S_w changes, the primary flow path for water is expected to be through the previously open oil paths, especially if little or no residual oil blocks the paths. However, if this were the case, F_{rrw} would not be expected to be 89 times greater than F_{rro}. On the other hand, the high water residual resistance factor could be explained if the paths closed up. Near the end of this paper, we will suggest that paths open during oil injection by partial dehydration of the gel. During subsequent water injection, the paths could partially close when the gel rehydrates.

Connectivity of Phases

Before Gel Placement, the Injected Phase Was Highly Connected. Using the new analysis, we determined the connectivity of the fluid phases in porous media. Not surprisingly, for all cases, nearly 100% of the injected phase was continuous or contained by the largest phase volume. This observation held regardless of the fluid that wetted the porous medium. (Details can be found in Ref. 3.) The fact that we could detect that nearly 100% of the injected phase was connected suggests that few very thin films were associated with the injected phase—whether it was the wetting phase or not. Since our voxel size was 4.1 μm, most films and connecting bridges must have been greater than 4.1 μm.

Most Residual Non-Wetting Blobs Were "Singlets". In Berea at S_{or} before gel placement, 57% of the residual oil blobs were "singlets," where each oil blob was associated with only one pore (Fig. 18). Similarly, in porous polyethylene at S_{wr} before gel placement, 66% of the residual water blobs were singlets. These findings are consistent with previous

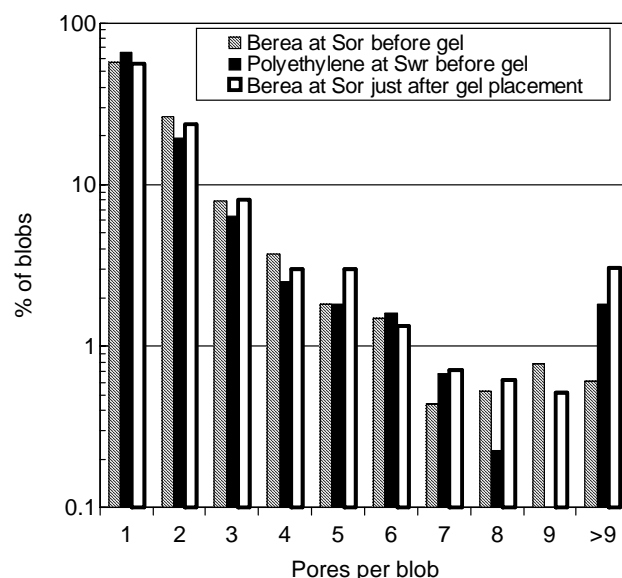microscopic analysis of residual oil in bead packs, where 65% of the blobs reportedly were singlets.[7]

Fig. 18—Residual phase blob distributions.

In Berea, we found 26% of the residual oil blobs were "doublets" (at S_{or} before gel placement), where each blob was distributed between two pores (Fig. 18). Similarly, in porous polyethylene (at S_{wr} before gel placement), 19% of the residual water blobs were doublets. For comparison, Chatzis *et al.*[7] quoted 20% of residual oil blobs were doublets in bead packs.

The fractions of blobs with greater numbers of pores per blob are shown in Fig. 18. The largest residual non-wetting-phase blob (before gel placement) involved 25 pores per blob in Berea and 20 pores per blob in porous polyethylene. In Berea, the largest oil blob (0.00654 mm³) accounted for 1.76% of the total residual water phase (within the small image volume). In polyethylene at S_{wr}, the largest water blob (0.0204 mm³) accounted for 4.15% of the total residual water phase.

In both Berea and polyethylene, the average pore size involved with triplets and doublets was about the same as that involved with singlets. For blobs with larger numbers of pores, the average pore size was typically two to three times the average pore size associated with the singlets.

Since oil was mobilized during gelant placement, we wondered whether the blob distribution was changed by the placement process. The blob distribution in Berea at S_{or} immediately after gel placement is shown by the white bars in Fig. 18. A comparison with the hatched bars reveals that the distribution of blob sizes was little changed by the process of gel placement. The only significant difference was that gel placement induced the formation of a larger fraction of blobs that contained more than 9 pores (0.6% before gel placement versus 3.1% just after gel placement).

Were Residual Wetting Blobs Connected by Thin Films? For a strongly-wetted porous medium, the residual wetting phase was expected to be nearly all connected. In other words, we expected a single water blob to exist at S_{wr} in strongly water-wet Berea or a single oil blob to exist in strongly oil-wet

polyethylene at S_{or}. In polyethylene, the largest detected oil blob contained 36.2% of the total oil volume at S_{or1} and 46.1% of the total oil volume at S_{or2}. Since the oil films were extremely thin (nanometer thicknesses) and our voxel size was 4.1 μm, we probably did not detect many of the connections between the residual oil blobs. The same logic likely applies to residual water blobs in Berea. The largest detected water blob accounted for 5.0% of the residual water in Berea at S_{wr}. Presumably, thin undetected water films connect most of the residual water blobs in Berea. Considering the results in the previous section, connecting films must be thicker when the wetting phase was injected than when it was residual.

After Gel, the Injected Phase Was Highly Connected. For all cases after gel placement, the largest detected blob for the injected phase contained a substantial portion of the total phase volume. In Berea at S_{wr} after gel, the oil saturation was 71.3%, and 96.1% of the injected oil was connected. This value emphasizes the widespread reduction of gel volume by oil throughout the image volume. Assuming that gel occupied all of the aqueous pore space when placed (63.7% from Table 1), oil injection destroyed 55% of the gel (35 saturation point increase in oil saturation). Fig. 12 suggests some resistance to gel destruction in the small- to moderate-sized pores (because many of these pores had post-gel water saturations that were greater than before gel). However, the figure also shows that for all size ranges, many pores had nearly the same saturations after gel as before gel. Presumably, gel formed in the aqueous pore space in most (if not all) pores. Therefore, oil injection caused widespread reduction in gel volume in most pores in order to reach S_{wr} after gel (Fig. 10).

During water injection after gel placement in Berea, the final water saturation was 49.0%, and 80.5% of the aqueous phase was connected within the largest blob. Although some water volume was contained in smaller blobs, we cannot discount the possibility that these blobs may be connected through thin undetected water films that follow pore walls. Also, our use of XMT cannot distinguish between free water and gel. Since the water saturation at S_{wr} was 28.7% after gel placement, the final gel saturation may have been as high as 28.7%. Assuming that the gel did not swell during final water injection, the free water saturation at S_{or} after gel could have been at least 20.3% (i.e., 49.0%-28.7%).

During oil injection after gel placement in polyethylene, the final oil saturation was 16.5%, and 45.5% of the hexadecane oil was contained by the largest blob. Again, we suspect that most of the smaller blobs were connected by thin undetected oil films.

During water injection after gel placement in polyethylene, the final water saturation was 99.7%, and 99.98% of that water was connected. Since S_{wr} during the prior oil injection was 83.5%, the final gel saturation may have been as much as 83.5% and the free water saturation may have been 16.2% (i.e., 99.7%-83.5%).

After Gel, the Residual Phases Were Highly Connected. The most interesting observation during water injection after gel placement in Berea was that the residual oil was highly connected. S_{or} after gel placement was 51.0%, and 77.6% of that oil was contained within the largest oil blob. This blob

was 122 times larger than the largest oil blob at S_{or} before gel placement. This high degree of connection helps explain the relatively high permeability to oil after gel placement.

For water at S_{wr} in Berea after gel placement, the water saturation was 28.7%, and 25.7% of this water was included in the largest residual water blob. Since water was the wetting phase, we suspect that most (if not all) of the aqueous phase was actually connected, but that our XMT technique was simply not able to detect the thin film connections along the pore walls. Even so, it is interesting that the connected volume (25.7% of the total 28.7% S_{wr}) was substantially larger than the connected volume noted at S_{wr} before gel placement (5.0% of the total 16.0% S_{wr}). Perhaps with the higher S_{wr} after gel placement, the connecting water film was thicker and easier to detect than before gel placement.

For oil at S_{or} in polyethylene after gel placement, the oil saturation was only 0.3%, and 32.3% of this oil was included in the largest residual oil blob. Since oil was the wetting phase, we suspect that most (if not all) of the oil phase was actually connected, but that our XMT technique was simply not able to detect the thin film connections along the pore walls. In view of the low oil saturation and the difficulty in seeing the connecting water films in Berea, it is somewhat surprising that we could detect a relatively large residual oil blob in polyethylene.

For water at S_{wr} in polyethylene after gel placement, S_w averaged 83.5%, and 99.8% of this water was connected. We suspect that this was probably one large gel blob.

Higher Saturations Resulted in Greater Connectivity. Injection of the 20-cp gelant mobilized oil—decreasing the oil saturation for polyethylene and increasing the oil saturation for the image volume for Berea. The changes in connectivity qualitatively followed the trends expected from the saturation changes. In Berea, gelant injection caused oil saturation in the image volume to increase from 18.4% to 36.3%, the largest oil blob grew from 1.76% to 11.8% of the total oil phase volume, and the largest water blob shrank from 97.9% to 95.0% of the total water phase volume. In polyethylene, gelant injection decreased oil saturation from 17% to 0.2%, the largest oil blob shrank from 46.1% to 4.23%, and the largest water blob grew from 99.8% to 99.985%.

The correlation between oil saturation and blob connectivity continued to hold during oil injection after gel formation. In Berea, oil injection after gel placement caused oil saturation in the image volume to increase from 36.3% to 71.3%, the largest oil blob grew from 11.8% to 96.1% of the total oil phase volume, and the largest water blob shrank from 95.0% to 25.7% of the total water phase volume. In polyethylene, oil injection after gel placement increased oil saturation from 0.2% to 16.5%, the largest oil blob grew from 4.23% to 45.5%, and the largest water blob contracted slightly from 99.985% to 99.78%. In summary, the largest oil blob always grew when the oil saturation increased and shrank when the oil saturation decreased. Similarly, the largest water blob always grew when the water saturation increased and shrank when the water saturation decreased.

Properties of the Largest Oil Blob in Berea at S_{or} after Gel. At S_{or} after gel placement in Berea, 77.6% of the oil in the

image volume was contained in the largest residual oil blob. That blob had parts in 73% of the pores in the image volume (1,588 out of 2,176 pores). Thus, the blob was very widespread. As mentioned, it was 122 times larger than the largest oil blob that was present before gel placement. The pores that were involved with the largest oil blob had nearly the same distribution of pore sizes and water saturations as for all Berea pores in the image volume. For pores that participated with the largest oil blob, the average water saturation was 45%, compared with 49% for all Berea pores in the image volume. The average pore size involved with the blob (8.2×10^{-4} mm^3) was slightly larger than the average Berea pore (6.2×10^{-4} mm^3).

Why should gel allow such a large oil blob to exist? We speculated that the gel located in the extremities of individual pores (i.e., near pore walls, especially in the vicinity of greatest pore radius) might reduce the effective pore radius to more closely match the effective throat radius. Thus, the effective pore body/pore throat aspect ratio could be reduced to allow residual oil to remain connected through multiple pores. (In other words, with a lower aspect ratio, residual oil drops would be less inclined to snap off and become trapped as "singlets" in individual pores, as occurs at S_{or} before gel placement.) This scenario is consistent with that suggested in Ref. 8. To test this hypothesis, we analyzed the largest oil blob (at S_{or} after gel placement) as if it were a porous medium (i.e., with the oil representing the pore space, and everything outside the oil blob acting as "rock"). We found the "pore bodies" in the oil blob had a size distribution that closely paralleled the distribution for the original Berea sandstone. The average and median "pore volumes" were 5.1×10^{-4} mm^3 and 1.8×10^{-4} mm^3, respectively, for the oil blob, and 6.2×10^{-4} mm^3 and 2.8×10^{-4} mm^3, respectively, for the original Berea.

The distributions of aspect ratios are compared in Fig. 19. Aspect ratio was defined as the effective pore radius divided by the effective throat radius. The effective pore radius was determined by assuming that the measured pore volume was spherical. The effective throat radius was determined by assuming that the measured throat area was circular. (In reality, although our pore volumes, throat areas, and shapes were known with reasonable accuracy, the pores were decidedly not spherical, and the throats were not circular.)

Contrary to our speculation, the gel did not reduce the effective pore body/pore throat aspect ratio. Instead, the average "aspect ratio" for the oil blob (5.5) was 31% greater than that for Berea sandstone (4.2). For Berea pores, the peak in the distribution occurs at values from 2 to 3. In contrast, for the oil blob, the distribution peaked at values from 5 to 10.

The increase in aspect ratio associated with the presence of the gel might suggest that gel had a greater propensity to reside in pore throats than in pore bodies. However, the increased aspect ratio seems inconsistent with the existence of the large residual oil blob. With greater aspect ratios, why did the large oil blob not break up into many smaller blobs? A possible explanation is that water did not have access (or had limited access) to most of the pore throats after gel placement. With limited or no access, free water could not accumulate in pore throats to cause snap-off and form smaller oil blobs. The affinity of the gel to retain water could also explain why free-water films did not form and break up the largest oil blob.
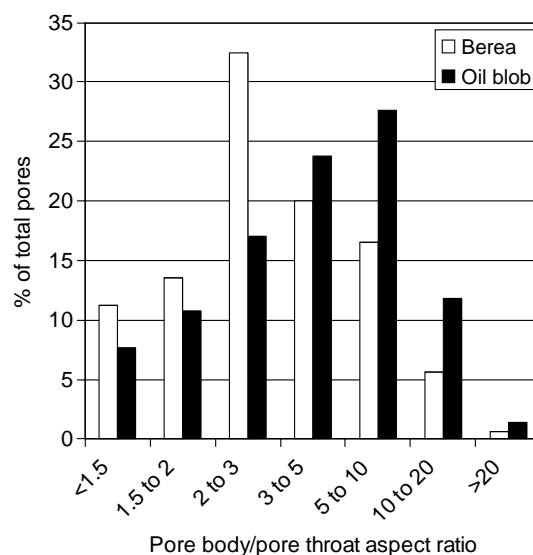

Fig. 19—Comparison of aspect ratios.

The distribution of coordination numbers for Berea and the largerst residual oil blob are compared in Fig. 20. Coordination number is the number of distinct exits from a given pore body. The average coordination number for "pores" in the oil blob (3.6) was 19% less than that for Berea sandstone (4.45). The peaks in the distributions occurred at a value of 3 in both cases. However, the oil blob had a much greater fraction of pores with low coordination numbers.
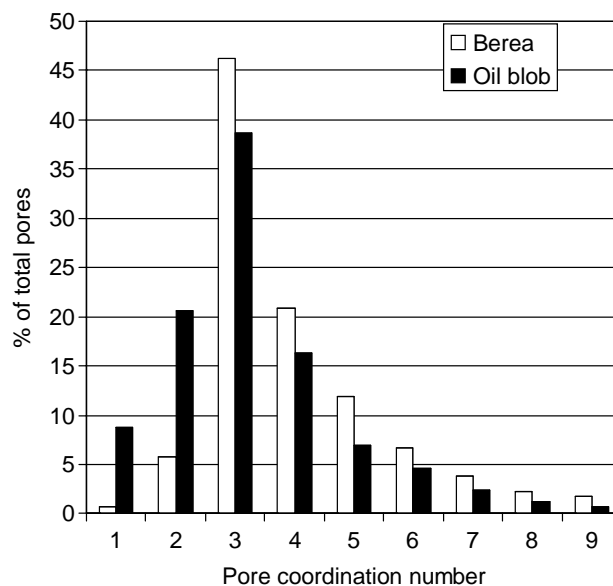

Fig. 20—Comparison of coordination numbers.

Mechanistic Implications

A key finding from our XMT studies was that oil injection reduced the pore volume that was occupied by gel. This reduction created pathways for oil flow, thus restoring an important level of permeability to oil. How did this reduction in gel volume occur? Several possibilities come to mind, including oil (a) ripping through the gel, (b) concentrating or dehydrating the gel, (c) mobilizing the gel, or (d) chemically

destroying the gel. Concerning the third possibility, pressure gradients were closely monitored during our experiments and were maintained well below the levels needed to mobilize gel. In addition, we have never observed gel production from our cores. Concerning the fourth possibility, our oil (hexadecane) is not reactive with any of the gel, brine, or rock components, so chemical destruction of the gel does not seem likely.

That leaves two mechanisms for active consideration. In one mechanism, oil ripped pathways through the gel.[1,2,9] In the second mechanism,[10,11] gel dehydrated (i.e., lost water and became more concentrated through compression.)

Our recent analysis supports the dehydration mechanism over the ripping mechanism. In particular, the apparent reduction in gel saturation during oil injection was insensitive to pore size in Berea (Fig. 10) and was greatest in small pores in porous polyethylene (Fig. 16). If ripping was the dominant mechanism, losses in gel volume should have been greatest in the largest pores. To explain, if gel failure (i.e., ripping) occurred at a gel-rock interface or within the gel, a force balance suggests that the pressure gradient for gel failure should be inversely proportional to the pore radius.[12,13] Thus, for a given applied pressure gradient, gel failure should occur dominantly in larger pores. Since this did not occur, our results argue against the ripping mechanism.

In contrast, the observed XMT results could be consistent with the dehydration mechanism. With a fixed pressure gradient applied through the porous medium, gel in all pores could be "squeezed" or dehydrated to the same extent, regardless of pore size.

Do Gels Rehydrate During Water Injection?

When water was reinjected to establish S_{or} after gel placement, gels conceivably could rehydrate and swell to some extent. Did this occur? Table 1 indicates that the water saturation (or the combined water plus gel saturation) in Berea changed from 63.7% immediately after gel placement, to 28.7% at S_{wr} after gel to 49% at S_{or} after gel. If the decrease in S_w from 63.7% to 28.7% during oil injection was entirely due to dehydration, the gel would have been concentrated by an average factor of 2.2. If the increase in S_w from 28.7% to 49% during water injection was entirely due to rehydration, the gel would have swelled by a factor of 1.7.

Table 1 also indicates that the water saturation (or the combined water plus gel saturation) in polyethylene changed from 99.8% immediately after gel placement, to 83.5% at S_{wr} after gel to 99.7% at S_{or} after gel. If the decrease in S_w from 99.8% to 83.5% during oil injection was entirely due to dehydration, the gel would have been concentrated by an average factor of 20%—much less than observed in Berea. If the increase in S_w from 83.5% to 99.7% during water injection was entirely due to rehydration, the gel would have swelled almost entirely back to its original size. Additional evidence of rehydration comes from the F_{rro} and F_{rrw} values for gel in the polyethylene core. The residual resistance factor increased from 24 during oil injection to 2,130 during brine injection. Since our earlier discussion suggested that oil and water may largely follow the same path, the high F_{rrw} value could be explained by gel rehydration partially closing the path.

Conclusions

In previous work, we used X-ray computed microtomography to determine why a Cr(III)-acetate-HPAM gel reduces permeability to water more than that to oil in strongly water-wet Berea sandstone and strongly oil-wet porous polyethylene cores. Our X-ray images were re-analyzed using a different method for segmenting the fluids (i.e., differentiating between water and oil). The following conclusions were reached.

1. During the transition from S_{wr} to S_{or} in Berea before gel placement, pores in all detected size ranges experienced significant gains in water saturation. Pore size did not significantly influence the extent of the transition.
2. In contrast, in polyethylene before gel placement, oil was largely immobile in smaller pores.
3. Injection of our 20-cp gelant mobilized oil in both porous media even though the pressure gradients during gelant placement were less than those during previous floods.
4. Immediately after gel placement, an extremely high resistance (F_{rrw}>10,000) to water flow occurs (in either Berea or polyethylene), presumably because impermeable gel occupies nearly all of the aqueous pore space.
5. During oil flow after gel placement in Berea, much of the gel was destroyed or experienced a reduction in volume, thus leading to a relatively high permeability to oil (F_{rro}=15). A 55% reduction (on average) in gel volume occurred in pores of all detected size ranges. Gel volume was most likely to be reduced in pores that experienced the greatest saturation changes during floods before gel placement. After gel placement, 86.1% of the pores had higher S_{wr} values than before gel. Presumably, gel accounted for this increase. The gel that remained was widely distributed.
6. At S_{or} after gel placement in Berea, 93.3% of the pores had higher oil saturations than at S_{or} before gel placement. The overall S_{or} in Berea jumped from 18.4% before gel placement to 51% after. The greater level of trapped oil greatly restricted water flow (F_{rrw}=1,220). A wide range of saturation changes occurred for all pore sizes, and the average saturation change was insensitive to pore size.
7. In polyethylene, reduction in gel volume occurred mainly in small pores. Overall, oil injection apparently reduced gel volume by only 16.3%. However, for pores smaller than 10^{-4} mm^3, gel volume was reduced by 63.5%.
8. The above observations suggest that reduction in gel volume was probably caused by a dehydration mechanism rather than a gel-ripping mechanism.
9. In polyethylene, the overall S_{or} was significantly lower after gel placement than before gel placement (0.3% versus 17.0%). Thus, oil trapping could not explain the large disproportionate permeability reduction seen in porous polyethylene (F_{rrw}/F_{rro}=2,130/24=89). Gel rehydration provides a viable explanation.
10. Before gel placement, at least 97.9% of the injected phase (oil or water) was connected.
11. Before gel placement, most residual non-wetting blobs were "singlets"—i.e., isolated within individual pores.
12. Changes in blob connectivity qualitatively followed the trends expected from the saturation changes. The largest oil blob always grew when the oil saturation increased and

shrank when the oil saturation decreased. Similarly, the largest water blob always grew when the water saturation increased and shrank when the water saturation decreased.

13. In Berea at S_{or} after gel placement, 77.6% of the residual oil was contained within the largest blob. This blob was 122 times larger than the largest oil blob at S_{or} before gel placement. Based on consideration of aspect ratios, we were surprised that this large blob could exist. The affinity of gel for water may have limited the formation of water films that would be needed to break the large oil blob into small blobs.

Acknowledgments

Nomenclature

F_{rro} = oil residual resistance factor
F_{rrw} = water residual resistance factor
k_{ro} = relative permeability to oil
k_{rw} = relative permeability to water
S_{or} = residual oil saturation
S_{or1} = first residual oil saturation before gel
S_{or2} = second residual oil saturation before gel
S_w = water saturation
S_{wr} = connate or residual water saturation

References

1. Seright, R.S, Liang J., Lindquist, B.W., and Dunsmuir, J.H.: "Characterizing Disproportionate Permeability Reduction Using Synchrotron X-Ray Computed Microtomography," *SPEREE* (Oct. 2002) 355-364.

2. Seright, R.S, Liang J., Lindquist, B.W., and Dunsmuir, J.H.: "Use of X-Ray Computed Microtomography to Understand Why Gels Reduce Permeabilty to Water More Than That to Oil," *J. Petroleum Science and Engineering*, **39**, Nos. 3-4 (Sept. 2003) 217-230.

3. Seright, R.S.: "Conformance Improvement Using Gels," Annual Technical Progress Report (U.S. DOE Report DOE/BC/15316-4), U.S. DOE Contract DE-FC26-01BC15316 (Sept. 2003) 2-34.

4. Wang, D. *et al*: "Study of the Mechanism of Polymer Solution with Visco-Elastic Behavior Increasing Microscopic Oil Displacement Efficiency and the Forming of Steady Oil Thread Flow Channels," paper SPE 68723 presented at the 2001 SPE Asia Pacific Oil and Gas Conference and Exhibition, Jakarta, Indonesia, April 17-19.

5. Seright, R.S.: "Using Chemicals to Optimize Conformance Control in Fractured Reservoirs," Annual Technical Progress Report (U.S. DOE Report DOE/BC/15110-2), U.S. DOE Contract DE-AC26-98BC15110, (Sept. 1999) 21-28.

6. Seright, R.S.: "Effect of Rock Permeability on Gel Performance in Fluid-Diversion Applications," *In Situ* (1993) **17**, No. 4, 363-386.

7. Chatzis, I., Morrow, N.R., and Lim, H.T.: "Magnitude and Detailed Structure of Residual Oil Saturation," *SPEJ* (April 1983) 311-326.

8. Zaitoun, A. and Bertin, H.: "Two-Phase Flow Property Modifications by Polymer Adsorption," paper SPE 39631 presented at the 1996 SPE/DOE Improved Oil Recovery Symposium, Tulsa, OK, April 19-22.

9. Al-Sharji, H.H., *et al*.: "Pore-Scale Study of the Flow of Oil and Water through Polymer Gels," paper SPE 56738 presented at the 1999 SPE Annual Technical Conference and Exhibition, Houston, TX, Oct. 3-6.

10. Willhite, G.P., *et al*.: "Mechanisms Causing Disproportionate Permeability in Porous Media Treated With Chromium Acetate/HPAAM Gels," *SPEJ* (March 2002) 100-108.

11. Ganguly, S., *et al*.: "Effect of Flow Rate on Disproportionate Permeability Reduction," paper SPE 80205 presented at the 2003 SPE International Symposium on Oilfield Chemistry, Houston, TX, Feb. 5-7.

12. Liu, J., and Seright, R.S.: "Rheology of Gels Used For Conformance Control in Fractures," paper SPE 59318 presented at the 2000 SPE/DOE Improved Oil Recovery Symposium, Tulsa, OK, April 3-5.

13. Seright, R.S.: "Washout of Cr(III)-Acetate-HPAM Gels from Fractures," paper SPE 80200 presented at the 2003 SPE International Symposium on Oilfield Chemistry, Houston, TX, Feb. 5-7.

SI Metric Conversion Factors

cp x 1.0*	E-03	= Pa·s
ft x 3.048*	E-01	= m
in. x 2.54*	E+00	= cm
md x 9.869 233	E-04	= μm^2
psi x 6.894 757	E+00	= kPa

*Conversion is exact.